# TEM-CHARACTERIZATION OF METALLIC NANOPARTICLES EMBEDDED IN SOL-GEL PRODUCED GLASS-LIKE LAYERS

U. WERNER, M. SCHMITT, H. SCHMIDT
Institut für Neue Materialien, Im Stadtwald 43, D-66123 Saarbrücken, Germany

## ABSTRACT

Size and shape of metallic nanoparticles, which are embedded in sol-gel produced glass-like layers, are able to influence the optical properties of coatings on glass. Since the shape of the particles is determined by its crystalline structure, and the structure is modified significantly during the particle growth, the development of both was observed in dependence on the stage of growth applying conventional and high resolution electron microscopy. These investigations carried out on Au and Ag particles have revealed different types of colloidal growth, a real structure often formed by dislocations and twins as well as a relatively high particle mobility.

## INTRODUCTION

The embedding of metallic nanoparticles in glass-like layers, which are produced by sol-gel processing, allows the modification of the optical properties of these layers such as the optical absorption and the nonlinear optical properties. This modification is determined by the concentration, size, shape and the internal structure of the particles [1]. In order to improve the knowledge with respect to an optimum embedding, the electron-microscopical investigation aims especially at the characterization of vicinity, size, shape, internal structure and behavior of the nanoparticles, and the variation of these parameters during the particle growth. Comprehensive information is obtained by transmission electron microscopy (TEM) techniques starting from the global characterization of the layer using ordinary diffraction contrast up to the investigation of the atomic structure level of the nanoparticles using the interference contrast of high-resolution electron microscopy (HREM) at an acceleration voltage of 200 kV.

## EXPERIMENT AND PREPARATION

The synthesis of nanocrystalline Au and Ag particles [2], which are embedded in glass-like coatings, starts with an $SiO_2$ sol to which the corresponding metal is added in ionic form ($H[AuCl_4]$, $AgNO_3$). By using functionalized aminosilanes the metal ions are enabled by their complexation to go into solution and, simultaneously, their reduction is suppressed. Glass slides are covered with this organically modified $SiO_2$ sol by applying the dip-coating method. The metal ions are reduced by the electrons released during the decomposition and combustion of the organic sol components in the subsequent heating procedure (densification temperature: $T_d$ = 100-600°C). By this process the colloidal nucleation is initiated. An uncontrolled growth is prevented by the functionalized silanes which cover the colloid surfaces and thus avoid by their entropic interaction forces a premature coagulation and coalescence of the colloids. Additionally, the heating causes that the solvent of the sol evaporates, which leads to the development of an organic-inorganic (ormocer) or glass-like matrix (described in detail in [3,4]).

The embedding of the particles in an electrically insulating amorphous layer gives rise to unfavorable imaging conditions such as inelastic scattering of electrons (loss of coherence) and electrical charging of the layer (resulting in spontaneous specimen motions as well as astigmatism). These influences are minimized by extensively reducing the matrix material in two ways: firstly, the simple scratching off of layer splinters from the coatings on glass and, secondly, the ion beam etching of the covered glass slides. While the first case offers the advantage of easy structure imaging of nanoparticles positioned in the wedge-shaped edge region of the splinters, the second case offers the possibility to get relatively large electron transparent areas which allow survey images in diffraction contrast.

## RESULTS AND DISCUSSION

### The particle shell

The colloidal growth is decisively governed by the mutual repulsion of the ligands enveloping the nanoparticles. Hence, for the assessment of the growth a characterization of the ligand shells is eminently important. However, the amorphous ligand shells embedded in the ormocer matrix (where they are not yet decomposed by the heating procedure) show no directly observable electron microscopical contrast. The application of ion beam etching opens a way for their indirect observation because of the strength-sensitive material erosion by the ion beam: Since the ligand molecules have a catalytic effect on the hydrolysis and condensation, the densification of the matrix in the range of the ligand shells becomes higher than in the remaining region. By this process the ion beam can uncover the higher densified particle shells without dismantling them.

Fig. 1a shows an Ag nanoparticle with a stronger densified ormocer shell (thickness: 9.0 nm) in an ion beam thinned ormocer matrix ($T_d$ = 200°C) that was imaged with the incident electron beam parallel to the layer surface. The measured shell thickness within an extremely thin layer area - where the shells of relatively small particles also possess sufficient contrast - is depicted in the diagram of Fig. 1b. This diagram shows no systematic variation of the shell thickness in dependence on the particle diameter; the measurement yields a mean shell thickness of 7.5 nm. This behavior reveals the causal action of a shell forming process, such as the attachment of ligands to the particles and their catalytic effect during the densification of the $SiO_2$ network, which is independent of size and shape of the particles.

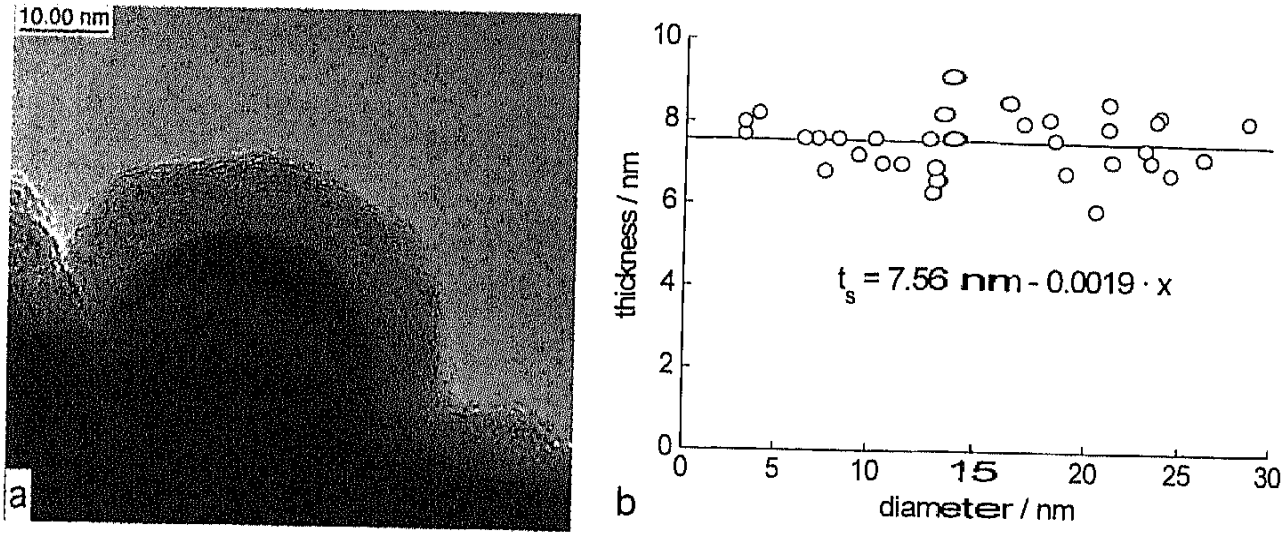


Fig. 1: a) Imaging of an enveloped Ag nanoparticle originally embedded in an ormocer matrix (Ag / aminosilane = 1 / 1, $T_d$ = 200°C) after [4]. The stronger densified ormocer shell of the particle was uncovered due to the strength-sensitive material erosion of an ion beam. b) Thickness of the shells $t_s$ depending on the particle diameter x. The fitted straight line ( $t_s$ = 7.56 nm - 0.0019 · x ) yields no variation of thickness as function of the diameter.

### Size distribution of the embedded particles

Using self-supporting organically modified $SiO_2$ layers (ormocer layers) with embedded Au colloids (Au / aminosilane = 1 / 4, $T_d$ = 120°C) investigations of size distributions of metallic nanoparticles were carried out. By means of ion beam etching it was possible to thin sufficiently large areas with negligible variation in thickness that allowed the imaging of a statistically representative number of particles. The size distributions for different times after the layer densification are shown in Figs. 2a and b: The fraction of larger particles with partly pronounced crystalline habit is clearly greater in Fig. 2b than in 2a. The reason for this aging process recorded here must be mainly attributed to the ormocer layer with its moderate densification. Similar processes are hardly taking place with the same high intensity in fully densified glass-like layers. However,

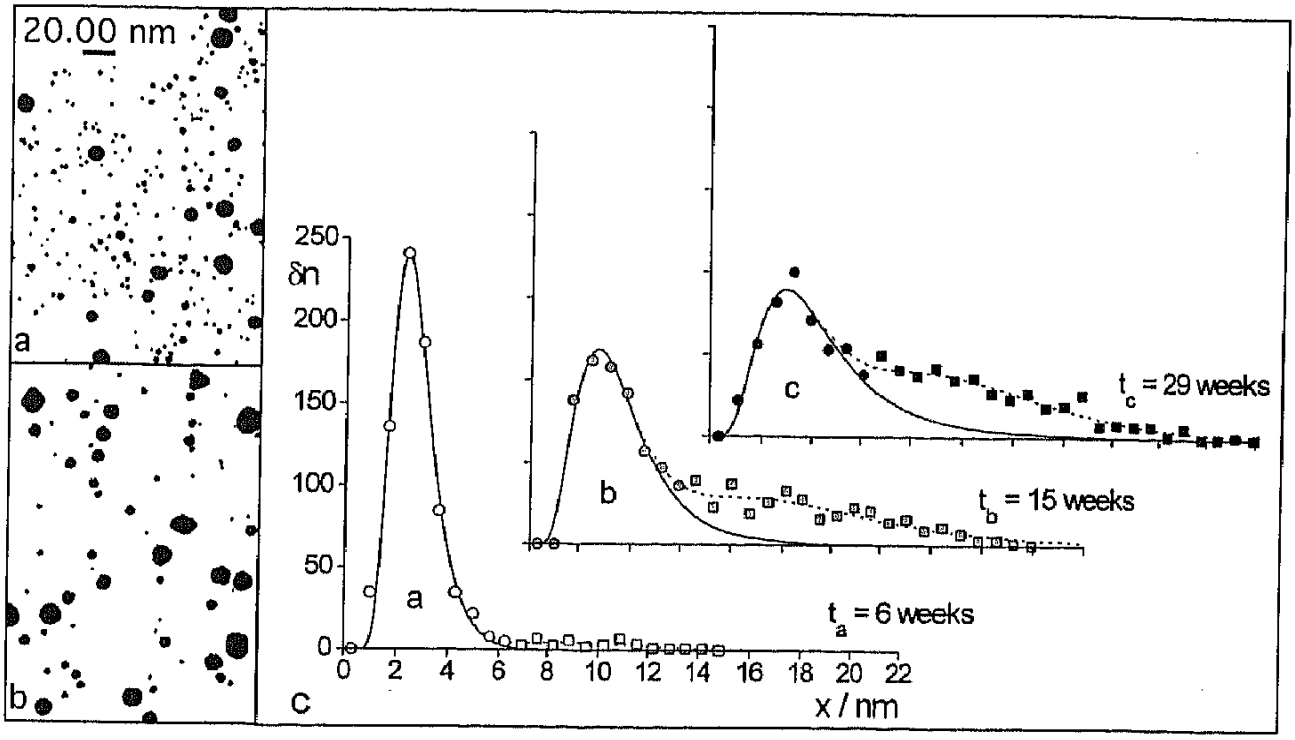


Fig. 2: Evolution of the size distribution of Au colloids in an ormocer layer (Au / aminosilane = 1 / 4, $T_d = 120°C$) determined 6 (image and graph a), 15 (image and graph b) and 29 weeks (graph c) after the densification (storage at room temperature). Fig. 2c: Particle number counted per class $\delta n = dn / dx \cdot \delta x$ ($\delta x$: width of classes) depending on the diameter x of the Au particles (because of different microscopical magnifications all graphs become absolutely comparable by multiplying $\delta n$ of graph 'a' by 3.6). Fitting of log-normal distributions (equation (1), solid lines) to the frequencies in the low-diameter region.

the investigation of the aging process permits interesting conclusions on the crystal growth in sol-gel produced matrices.

The binary images of Figs. 2a and b were derived from the originals by image processing procedures such as shading correction, pixel editing, binarization and opening. The obtained binary images permit a computer-aided evaluation regarding the size distributions given in the graphs of Fig. 2c. In the range of small particle diameters the diameter frequencies can be fitted by a log-normal distribution with positive skewness

$$\frac{dn}{dx} = \frac{n_0}{\sqrt{2\pi} \cdot \sigma x} \cdot \exp\left[ -\frac{(\ln x - \ln \xi)^2}{2\sigma^2} \right] \qquad (1)$$

with the parameters according to Table I.

Table I: Parameters of the log-normal distribution (1): x stands for the particle diameter, $N_0$ for the total particle number, $n_0$ for the particle number covered by the log-normal distribution and $\xi$ as well as $\sigma$ for the distribution parameters. The expectation value EX, standard deviation $\sqrt{D^2X}$ and skewness $\gamma$ of the distribution are also given.

| | t / weeks | $N_0$ | $n_0$ | $\xi$ / nm | $\sigma$ | EX /nm | $\sqrt{D^2X}$ /nm | $\gamma$ |
|---|---|---|---|---|---|---|---|---|
| $t_a$ | 6 | 793 | 728 | 2.57 | 0.326 | 2.71 | 0.91 | 1.04 |
| $t_b$ | 15 | 887 | 600 | 3.36 | 0.473 | 3.76 | 1.88 | 1.62 |
| $t_c$ | 29 | 894 | 576 | 3.95 | 0.546 | 4.58 | 2.70 | 1.86 |

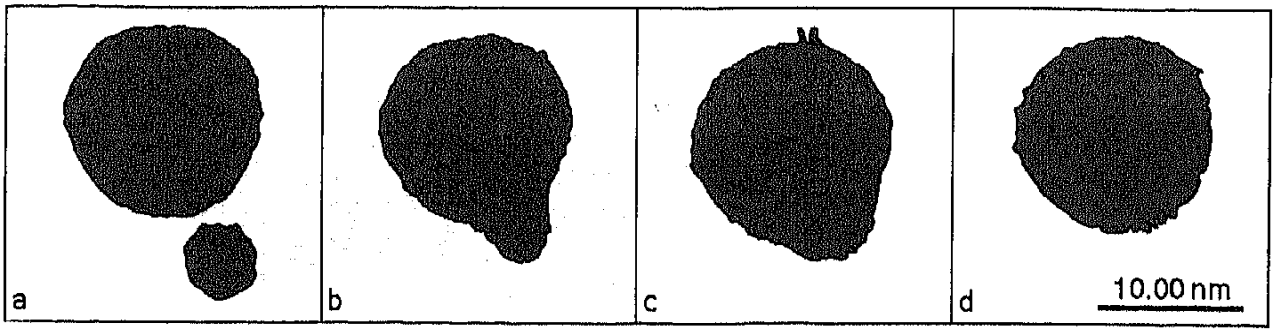


Fig. 3: Sequence of a liquid-like coalescence of two Au nanoparticles in a glass-like $SiO_2$ matrix (Au / aminosilane = 1 / 4, $T_d$ = 500°C). The particle fusion was initiated solely by the energy transferred by the imaging electron beam at a TEM dose rate < 50000 $e^-/nm^2$ per image. Image processing: contour tracing.

The development of a positively-skewed log-normal distribution points to a growth process that proceeds on the basis of a liquid-like particle coalescence [5]. The probability of such a process can be realized if one considers that the particles covered by the log-normal distribution have diameters clearly below 6 nm. Gold clusters of this size show a liquid-like behavior in vacuum above room temperature because of their lowered melting points [6]. Provided that this behavior, or at least an extremely easy modifiability of the internal structure applies to the embedded clusters, too - and the observed behavior indicates this (see Fig. 3) - the measured distributions can be interpreted as follows: During the densification of the matrix at a temperature of 120°C the growth of the majority of the initially formed gold crystal nuclei takes place via liquid-like coalescence. A pronounced log-normal distribution results as shown in the graph 'a' in Fig. 2c. This growth process probably continues also after the densification, however, in a much reduced way. This is indicated by the statistical mean and standard deviation of the log-normal distribution increasing with time (cf. graphs 2a-c). Particles with diameters > 6 nm distinctly deviate from the log-normal distribution. They are essentially formed a long time after densification ($T_d$ = 120°C) and show a partly pronounced crystal habit. An estimation of the volume fractions of the different groups of particles reveals that the growth of the larger ones cannot be attributed to the numerical shrinkage of the smaller ones (eventually by Ostwald ripening) because the whole volume of the larger particles exceeds that of the smaller ones to a large extent. However, since estimations have shown [7] that a great deal of the ionic Au (80%) was not reduced during the densification, it can be assumed that these ions were reduced during the aging of the matrix. Therefore, a growth by diffusion and absorption of reduced metal ions can be considered as the most obvious interpretation of the creation of the larger colloids.

Coalescence and internal structure of nanoparticles

Occasionally, particles embedded in glass-like matrices can be detected which are formed by coalescence, which however, neither reach an ideal equilibrium shape nor an irregular one. These particles show a needle-like shape with a preferred orientation as represented in Fig. 4. Such particles are technologically interesting due to their relatively high aspect ratio that causes nonlinear optical effects. For utilization of such particles a deeper understanding of their coalescence behavior and the internal structure of particles in glass-like layers is necessary.

Owing to the easy modifiability of the lattice structure of nanoparticles the energy transferred by a strongly focused intense electron beam can be sufficient to give rise to coalescence of particles. A structure image of a nanoparticle generated in this way by the fusion of two particles is shown in Fig. 5. In order to get an undisturbed insight into the crystalline structure the primary colloids were grown in solution controlled by ligands, and subsequently deposited onto a carbon film. Furthermore, for a clear representation of the crystalline structure a graphical computer-aided evaluation of the image via image processing was performed. This processing - represented in Fig. 6 - comprises a local contrast maximization in the image of the atomic rows, followed by image binarization and determination of the gravity centers of the rows of the atoms as well as, finally, a schematic drawing of the atomic rows and of (111) and (002) lattice planes.

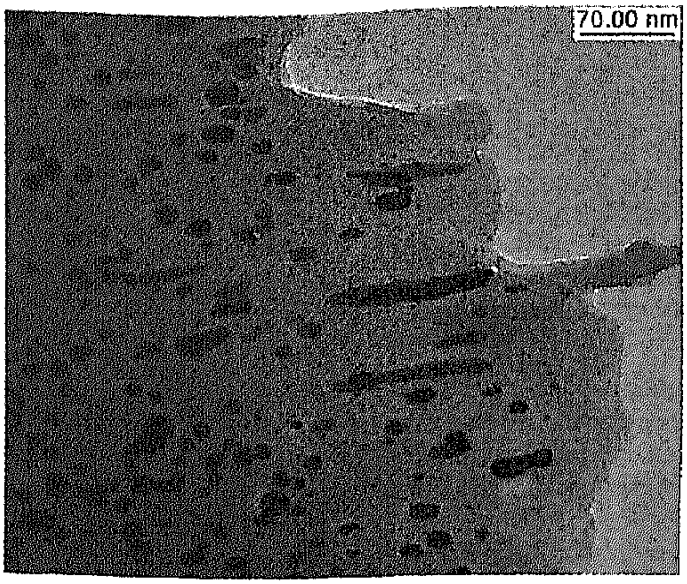


Fig. 4: Partially strongly oriented elongated Au particles (Au / aminosilane = 1 / 4, $T_d$ = 500°C) formed by coalescence in an area of a highly densified glass-like layer.

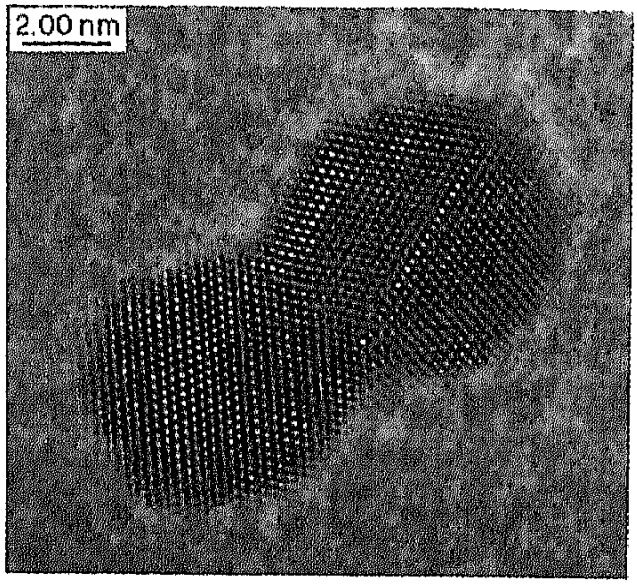


Fig. 5: Many beam imaging of a dumb-bell-shaped particle formed by intense electron irradiation induced coalescence of two Au colloids (Au / aminosilane = 1 / 10, grown in solution). Image processing: sum of the original image and its masked Fourier filtering.

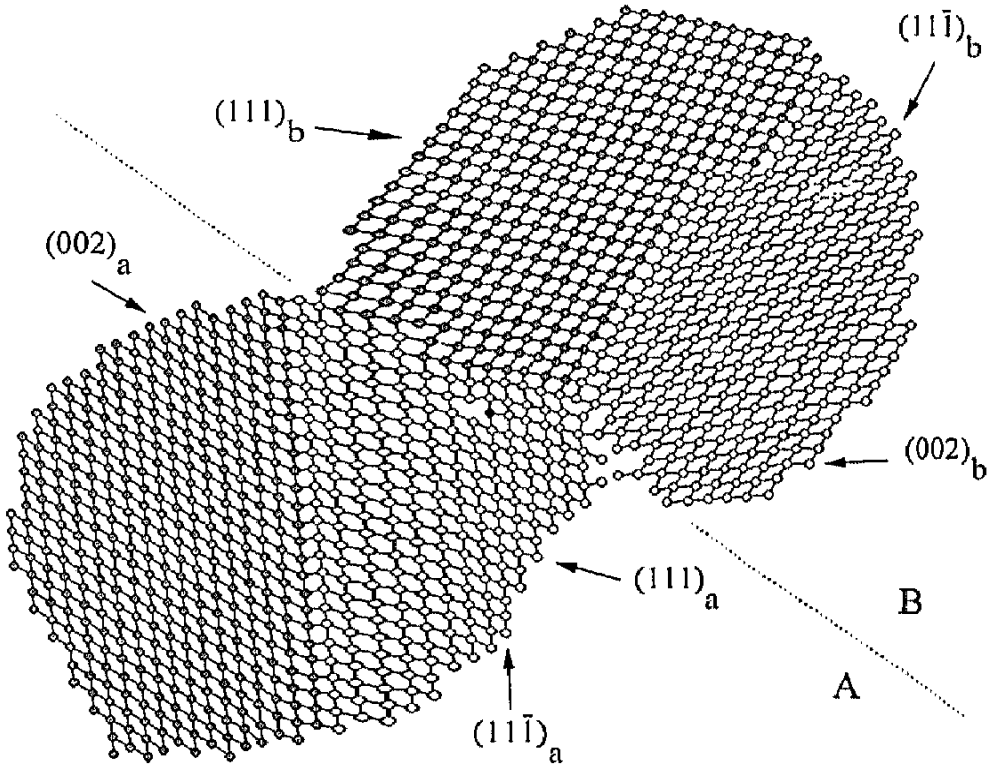


Fig. 6:

Graphical evaluation of Fig. 5 by the determination of the gravity centers of the atomic rows. The different grains are accentuated by different shading. The edge dislocation which compensates the misorientation between $(111)_a$ and $(111)_b$ lattice planes is marked by its black colored core.

The colloid shown in Fig. 6 was formed by two twinned primary particles. Initially their twin boundaries possessed an orientation difference of 25.5° and their centers of gravity were at a distance of 7.3 nm. During the course of the coalescence the particles have approached each other by 0.5 nm, and by this also rotated by 7.5°. As a result a fusion region was formed by a distorted twin boundary: E.g., the marked edge dislocation (dislocation core: black) compensates

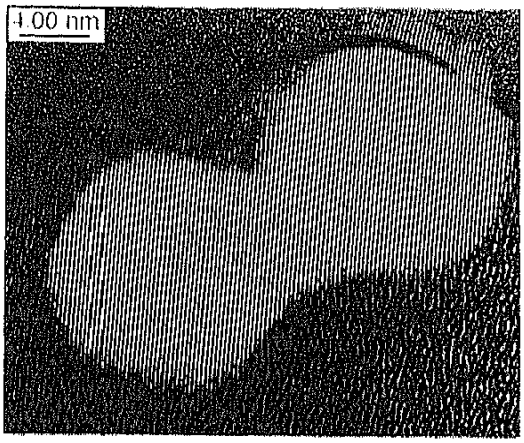


Fig. 7:

Dumb-bell-shaped particle with ideal lattice structure in the region of fusion formed by coalescence of two Au nanoparticles during densification of a glass-like coating (Au / aminosilane = 1 / 10, $T_d$ = 500°C). Image processing: sum of the original image and its masked Fourier filtering.

for the remaining misorientation between the $(111)_a$ and $(111)_b$ lattice planes of the primary particles A and B, respectively. The resulting coalesced particle has minimized its lattice energy essentially by rotating the primary particles and forming a twin boundary (as it has been observed in the case of particles produced by inert gas evaporation [8]) because a twin only insignificantly deviates from the ideal lattice structure.

The coalescence of two colloids during the densification of a glass-like coating is verified by Fig. 7 (unfortunately, due to electrical charging the image is affected by astigmatism). The resulting shape of the particle is also dumb-bell-like and the imaged (111) lattice fringes exhibit no distortions in the contact region. This ideal fusion of the lattice structure of both primary particles suggests that an adaptation of the orientation of the particles by rotation must have preceded the coalescence within the matrix, too; otherwise, an ideal fusion would be very improbable.

## CONCLUSIONS

The microscopic investigations of metallic colloids embedded in glass-like coatings have shown a stronger densification of glass-like particle shells caused by the growth-controlling ligand envelopes of the colloids. The observed positively asymmetric log-normal size distribution of the nanoparticles have revealed that in the densification process the crystalline particles mainly grow by means of liquid-like coalescence. On the basis of diffusion and condensation of metal atoms another growth process occurred as a result of aging of the investigated ormocer layer. Furthermore, the examinations have exhibited a relatively high mobility of the nanoparticles outside, but also inside the glass-like layer. This mobility comprises translational and rotational motions of the particles. It is assumed that the ability of the particles to carry out these motions combined with special conditions for these motions forced by the matrix structure during the densification could be the key to the understanding of the observed oriented coalescence of colloids forming highly elongated particles.

## REFERENCES

1. U. Kreibig in Contributions of cluster physics to material science, edited by J. Davenas and P.M. Rabette (Dordrecht: Nijhoff 1986), pp. 373-423.
2. M. Mennig, M. Schmitt, U. Becker, G. Jung and H. Schmidt, Sol-Gel Optics III, SPIE **2288**, 131-139 (1994).
3. M. Mennig, U. Becker, M. Schmitt and H. Schmidt, Advances in Science and Technology **11**, 39-46 (1995).
4. Cl. Fink-Straube, PhD thesis, Saarbrücken, 1994.
5. C.G. Granqvist and R.A. Buhrman, J. Appl. Phys. **47**, 2200-2219 (1976).
6. Ph. Buffat and J.-P. Borel, Phys. Rev. A **13**, 2287-2298 (1976).
7. B. Kutsch, O. Lyon, M. Schmitt, M. Mennig and H. Schmidt, to be published 1996.
8. P. Gao and H. Gleiter, Acta metall. **35**, 1571-1575 (1987).